UNIVERSITY OF AMSTERDAM

UvA-DARE (Digital Academic Repository)

Phosphinine-Based Ligands in Gold-Catalyzed Reactions

Rigo, M.; Habraken, E.R.M.; Bhattacharyya, K.; Weber, M.; Ehlers, A.W.; Mézailles, N.; Slootweg, J.C.; Müller, C.

DOI
10.1002/chem.201900938

Publication date
2019

Document Version
Final published version

Published in
Chemistry-A European Journal

License
Article 25fa Dutch Copyright Act

Link to publication

Citation for published version (APA):
Rigo, M., Habraken, E. R. M., Bhattacharyya, K., Weber, M., Ehlers, A. W., Mézailles, N., Slootweg, J. C., & Müller, C. (2019). Phosphinine-Based Ligands in Gold-Catalyzed Reactions. *Chemistry-A European Journal*, *25*(37), 8769-8779. https://doi.org/10.1002/chem.201900938

General rights
It is not permitted to download or to forward/distribute the text or part of it without the consent of the author(s) and/or copyright holder(s), other than for strictly personal, individual use, unless the work is under an open content license (like Creative Commons).

Disclaimer/Complaints regulations
If you believe that digital publication of certain material infringes any of your rights or (privacy) interests, please let the Library know, stating your reasons. In case of a legitimate complaint, the Library will make the material inaccessible and/or remove it from the website. Please Ask the Library: https://uba.uva.nl/en/contact, or a letter to: Library of the University of Amsterdam, Secretariat, Singel 425, 1012 WP Amsterdam, The Netherlands. You will be contacted as soon as possible.

UvA-DARE is a service provided by the library of the University of Amsterdam (https://dare.uva.nl)

Download date:09 Mar 2023

ChemPubSoc Europe
DOI: 10.1002/chem.201900938
CHEMISTRY A European Journal
Full Paper

Gold Catalysis |*Hot Paper*|

Phosphinine-Based Ligands in Gold-Catalyzed Reactions

Massimo Rigo,[a] Evi R. M. Habraken,[b] Koyel Bhattacharyya,[c] Manuela Weber,[a] Andreas W. Ehlers,[b, d] Nicolas Mézailles,[c] J. Chris Slootweg,[b] and Christian Müller*[a]

Dedicated to Professor Lothar Weber on the occasion of his 75th birthday

Abstract: A series of substituted phosphinines, 1-phosphabarrelenes and 5-phosphasemibullvalenes were synthesized and evaluated for their potential application as ligands in homogeneous catalytic reactions. While their buried volume (%V_{bur}) was calculated to get insight into the steric properties, [LNi(CO)$_3$] complexes were prepared in order to determine the corresponding Tolman electronic parameter. ETS-NOCV (extended-transition-state natural orbital for chemical valence) calculations on [LAuCl] complexes further allowed an estimation of the σ- and π-contributions to the L–M interaction. Au^I coordination compounds of selected examples were prepared and characterized by single crystal X-ray diffraction. Finally, the three classes of P^{III} compounds were successfully used in the Au^I-catalyzed cycloisomerization of *N*-2-propyn-1-ylbenzamide, showing very good activities and selectivities, which are comparable with the reported data of cationic phosphorus-based gold catalysts.

Introduction

Since the first successful preparation of phosphinines (**I**, Figure 1) by Märkl and Ashe, the rich and fascinating coordination chemistry of these aromatic phosphorus heterocycles has been explored extensively during the last decades.[1,2] In 1996, Zenneck and co-workers reported on the first application of a phosphinine-based catalyst in the [2+2+2]-cyclotrimerization of alkynes.[3] Since then the π-accepting ligand properties of phosphinines have been explored in several catalytic reactions, such as hydroformylations, (transfer-)hydrogenations, hydrosilylations, ethylene oligomerizations, hydroborations, cycloadditions and cycloisomerizations[2g,j,k,4] The formal [4+2]-cycloaddition reaction of phosphinines with activated alkynes leads to the formation of 1-phosphabarrelenes, the phosphorus congeners of barrelenes, according to the isolobal principle (**II**, Figure 1).[5] The incorporation of a phosphorus atom into the rigid [2.2.2]-bicyclic framework causes a strong pyramidalization of the donor atom, resulting in a lower σ-character of the P-lone pair along with a more pronounced π-accepting capacity of the ligand compared to a classical triarylphosphine.[5g,l]

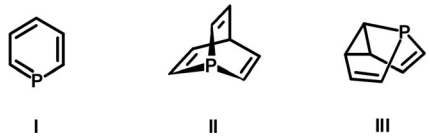

Figure 1. Phosphinine (**I**), 1-phosphabarrelene (**II**) and 5-phosphasemibullvalene (**III**).

1-Phosphabarrelenes have already shown excellent performance as P^{III} ligands in various transition-metal-catalyzed reactions, such as hydroformylations and C–C cross-coupling reactions.[5g–i,k,m–p] In 2017, we reported on the quantitative and selective photochemical di-π-methane rearrangement of 1-phosphabarrelenes into 5-phosphasemibullvalenes, the isolobal phosphorus analogues of semibullvalenes (**III**, Figure 1).[6] It turned out that these novel, rigid phosphorus cages have electronic properties similar to 1-phosphabarrelenes. However, the application of 5-phosphasemibullvalenes as ligands in homogeneous catalysis remains so far elusive. We also recently reported on 2,4,6-triarylphosphinine-based Au^I complexes, which were used for the first time in the Au^I-catalyzed cycloisomerization of dimethyl 2-(3-methylbut-2-enyl)-2-(prop-2-ynyl)malonate and the more challenging substrate *N*-2-propyn-1-ylbenzamide.[4e] We found that the phosphinine-based catalytic system is more active and selective than the Au^I complex containing a related, but strongly σ-donating mesoionic carbene as ligand. This prompted us to investigate and to evaluate in

[a] Dr. M. Rigo, M. Weber, Prof. Dr. C. Müller
Institut für Chemie und Biochemie
Freie Universität Berlin
Fabeckstrasse 34–36, 14195 Berlin (Germany)
E-mail: c.mueller@fu-berlin.de

[b] E. R. M. Habraken, Dr. A. W. Ehlers, Dr. J. C. Slootweg
Van't Hoff Institute of Molecular Sciences
Universiteit van Amsterdam
Science Park 904, 1090 GD Amsterdam (The Netherlands)

[c] Dr. K. Bhattacharyya, Dr. N. Mézailles
Systèmes de Hautes Energies
Université Paul Sabatier
118 route de Narbonne, 31062 Toulouse Cedex 9 (France)

[d] Dr. A. W. Ehlers
Department of Chemistry, Science Faculty
University of Johannesburg
P.O. Box 254, 2092 Auckland Park, Johannesburg (South Africa)

Supporting information and the ORCID identification numbers for some of the authors of this article are available on the WWW under https://doi.org/10.1002/chem.201900938.

© 2019 Wiley-VCH Verlag GmbH & Co. KGaA, Weinheim

detail the application of phosphinines, 1-phosphabarrenelenes and 5-phosphasemibullvalenes in Au^{I}-catalyzed cycloisomerization reactions.

Results and Discussion

Phosphinines **1** and **2** were prepared by the classical pyrylium salt route and from the corresponding 1,3,2-diazaphosphinine, respectively (Figure 2).[1a,7] The [4+2]-cycloaddition reaction of **1** and **2** with in situ generated benzyne affords the literature-known 1-phosphabarrelene **3** and the new 1-phosphabarrelene **4**.[5g] The bis(trifluoromethyl)-substituted 1-phosphabarrelene **5** was prepared by a modified literature procedure from **1** and hexafluoro-2-butyne, which allowed an easier purification from unreacted 2,4,6-triphenylphosphinine.[5a] 1-Phosphabarrelene **6** was obtained by heating a toluene solution of **2** to 60 °C for 16 h in the presence of an excess of hexafluoro-2-butyne. Compound **6** shows a quartet ($^{3}J(P,F) = 29.4$ Hz) in the $^{31}P\{^{1}H\}$ NMR spectrum at $\delta = -50.6$ ppm, which confirms the coupling between the phosphorus and the three adjacent fluorine atoms. Recrystallization from methanol afforded pure **6** as a white solid in 85% isolated yield. 5-Phosphasemibullvalenes **7** and **8** are formed quantitatively and selectively as a racemic mixture in a photochemical di-π-methane rearrangement from **3** and **4** and were obtained as pale-yellow solids after removal of the solvent. **7** and **8** show resonances in the $^{31}P\{^{1}H\}$ NMR spectrum at $\delta = 33.1$ ppm and $\delta = 49.0$ ppm, respectively (Figure 2). The di-π-methane rearrangement of **5** and **6** turned out to be unselective and led to a mixture of several trifluoromethyl-substituted products, which were not separated.[8]

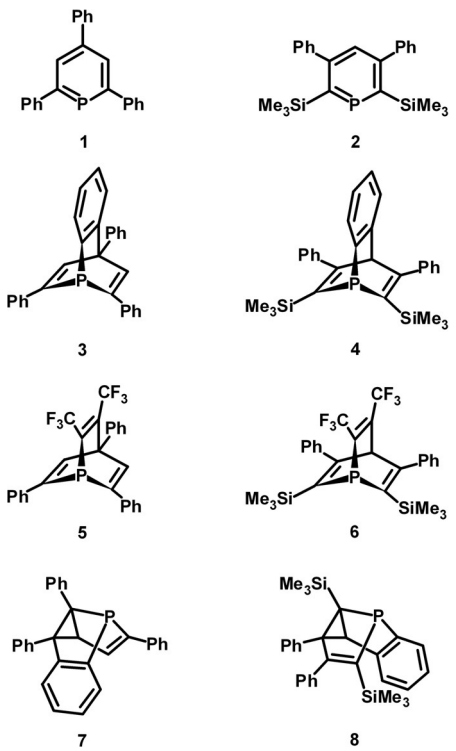

Figure 2. Phosphinine-based ligands **1**–**8**.

Single crystals suitable for X-ray analysis were obtained for 1-phosphabarrelenes **4** and **6** by slow evaporation of the solvent from concentrated solutions of the compounds in methanol. The molecular structures in the crystals are depicted in Figures 3 and 4, along with selected bond lengths and angles. Except for the interatomic distance C(18)–C(19), all bond lengths within the [2.2.2]-bicycle are slightly longer compared to the reported values found for **3**. Thus, the pyramidalization of the phosphorus atom in **4** is with $\Sigma\measuredangle(CPC) = 286.9°$ less strong than in **3** ($\Sigma\measuredangle(CPC) = 283°$), which suggests that the σ-donating properties of the $Si(CH_3)_3$-substituted **4** are higher than for the aryl-substituted 1-phosphabarrelene **3** (PPh_3: $\Sigma\measuredangle(CPC) = 308°$). According to the Walsh diagram of a phosphine PR_3, both the HOMO (lone pair) and the LUMO energy markedly fall in energy upon deformation of the phosphine

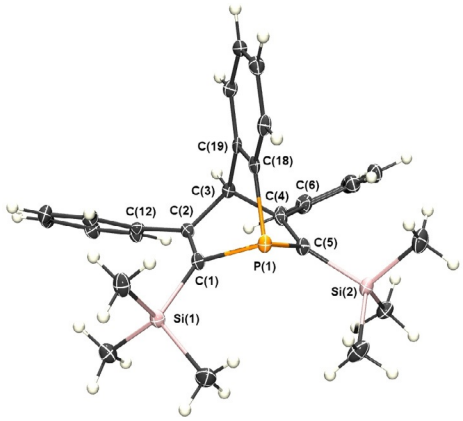

Figure 3. Molecular structure of **4** in the crystal. Displacement ellipsoids are shown at the 50% probability level. Selected bond lengths [Å] and angles [°]: P(1)–C(1) 1.868(3), P(1)–C(5) 1.869(3), P(1)–C(18) 1.842(3), C(1)–C(2) 1.344(3), C(2)–C(3) 1.538(3), C(3)–C(4) 1.538(3), C(4)–C(5) 1.343(4), C(18)–C(19) 1.402(3), C(19)–C(3) 1.517(3), Si(1)–C(1) 1.874(3), Si(2)–C(5) 1.881(3), C(1)-P(1)-C(5) 97.0(1), C(1)-P(1)-C(18) 94.9(1), C(5)-P(1)-C(18) 95.0(1).

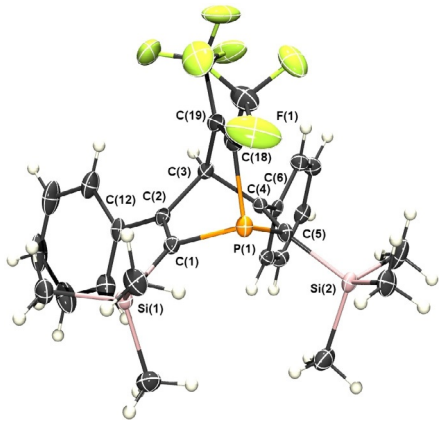

Figure 4. Molecular structure of **6** in the crystal. Displacement ellipsoids are shown at the 50% probability level. Only one independent molecule is shown. Selected bond lengths [Å] and angles [°]: P(1)–C(1) 1.869(2), P(1)–C(5) 1.864(2), P(1)–C(18) 1.858(2), C(1)–C(2) 1.341(3), C(2)–C(3) 1.544(3), C(3)–C(4) 1.544(2), C(4)–C(5) 1.338(3), C(18)–C(19) 1.328(3), C(19)–C(3) 1.520(3), Si(1)–C(1) 1.883(2), Si(2)–C(5) 1.881(2), C(1)-P(1)-C(5) 96.75(8), C(1)-P(1)-C(18) 94.16(9), C(5)-P(1)-C(18) 95.53(8).

© 2019 Wiley-VCH Verlag GmbH & Co. KGaA, Weinheim

from a planar to a pyramidal structure. Consequently, the phosphine becomes a less good σ-donor, but a better π-acceptor as it becomes more pyramidal.[5g,9]

The situation is comparable with the bis-CF_3-substituted 1-phosphabarrelene **6**. All bond lengths within the [2.2.2]-bicycle of **6** are very similar to the ones found for **4**, except for the interatomic distance C(18)–C(19), which is with 1.328(3) Å considerably shorter than in **4** (1.402(3) Å). Nevertheless, the pyramidalization found for the phosphorus atom in **6** is with $\Sigma\measuredangle$(CPC) = 286.5° almost identical to the value found for **4**.

Unfortunately, we were not able to obtain any crystallographic data on the 5-phosphasemibullvalenes **7** and **8**. However, compound **8** could easily be converted quantitatively into the corresponding selenide (**8** = **Se**) upon reaction with an excess of grey selenium, subsequent filtration and removal of the solvent. **8** = **Se** shows a single resonance at δ = 69.1 ppm in the $^{31}P\{^1H\}$ NMR spectrum with characteristic satellites and a phosphorus-selenium coupling constant of ^1J(P,Se) = 784.3 Hz. Single crystals suitable for X-ray diffraction were obtained by slow evaporation from a saturated solution of **8** = **Se** in toluene. The molecular structure of **8** = **Se** in the crystal, along with selected bond lengths and angles, is depicted in Figure 5 and allows a direct comparison with the crystallographically characterized selenide **7** = **Se**.[6]

The P–C bond lengths in **8** = **Se** are very similar to the values found for **7** = **Se**, while the bond length of P=Se (2.098(1) Å) is slightly longer in **8** = **Se** than in **7** = **Se** (2.0814(6) Å). The C(4)–C(3), C(3)–C(2) and C(2)–C(1) bond lengths in **8** = **Se** are slightly longer compared to corresponding values found for **7** = **Se**. Thus, the pyramidalization of the phosphorus atom is with $\Sigma\measuredangle$(CPC) = 289.9° smaller than the situation in **7** = **Se** ($\Sigma\measuredangle$(CPC) = 286°). This should result in a higher p-character of the phosphorus lone pair in **8**, which is also in line with a smaller ^1J(P,Se) coupling constant (^1J(P,Se) = 824.9 Hz versus 784.3 Hz).[10] Therefore, 5-Phosphasemibullvalene **8** should show slightly better σ-donating properties as **7**.

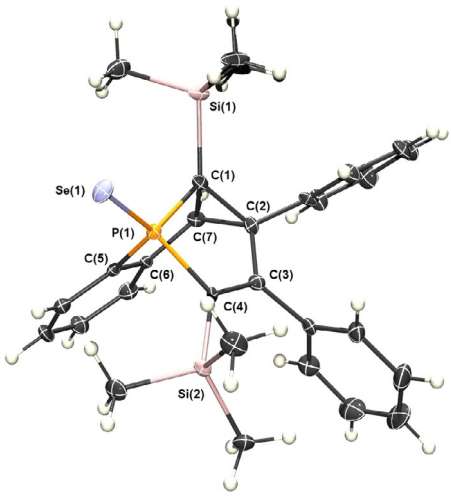

Figure 5. Molecular structure of **8** = **Se** in the crystal. Displacement ellipsoids are shown at the 50% probability level. Selected bond lengths [Å] and angles [°]: P(1)–C(1) 1.839(5), P(1)–C(4) 1.817(5), P(1)–C(5) 1.805(5), P(1)–Se(1) 2.098(1), C(1)–C(2) 1.526(7), C(1)–C(7) 1.526(6), C(1)–Si(1) 1.880(5), C(2)–C(7) 1.552(7), C(2)–C(3) 1.496(7), C(3)–C(4) 1.361(7), C(4)–Si(2) 1.877(5), C(5)–C(6) 1.398(7), C(6)–C(7) 1.499(7), C(1)-P(1)-C(5) 94.8(2), C(1)-P(1)-C(4) 96.22(2), C(4)-P(1)-C(5) 98.7(2).

Next, we started to evaluate the steric properties of compounds **1**–**8**. Several concepts have been developed during the last decades to describe the steric bulk of a ligand, especially with respect to applications in catalysis. In this respect, Tolman cone angle (θ) is probably the most widely used parameter.[11] The steric properties of phosphinines have so far mainly been described using the occupancy angles α and β.[12] However, this method only allows an estimation of the steric bulk of flat heterocycles and is, therefore, not suitable for a comparison with classical phosphine ligands. Even though 1-phosphabarrelenes are commonly regarded as bulky ligands, their steric properties have not been studied and compared so far. The same applies to 5-phosphasemibullvalenes, which are a completely new class of ligands. Another method for the evaluation of the steric hindrance of a given ligand is the calculation of the corresponding buried volume (%V_{bur}).[13] This descriptor, developed by the groups of Nolan and Cavallo, is the volume occupied by the atoms of the ligand (van der Waals radii) in a sphere of r = 3.5 Å. The ligand is computed at an interatomic distance of 2.00 or 2.28 Å from the metal center without considering the hydrogen atoms. %V_{bur} can be used for both planar and three-dimensional ligands, which allows a better comparison between structurally different ligands. A large number of data for common phosphorus-containing compounds and N-heterocyclic carbenes have been reported and were obtained from the corresponding gold complexes of the type [(**L**)AuCl].[14] These values can be calculated using a software developed by Cavallo et al., which is also able to calculate topographic steric maps.[15] Because of their relatively different shape, we decided to use this methodology for a comparison between phosphinines, 1-phosphabarrelenes and 5-phosphasemibullvalenes. Table 1 summarizes the calculated %V_{bur} values for compounds **1**–**8**, with the ligand located at an intermolecular distance of d = 2.28 Å from the center of a sphere with r = 3.50 Å.

Table 1. Calculated buried volumes (%V_{bur}) for compounds **1**–**8**.

	1	2	3	4	5	6	7	8
%V_{bur}	29.2	38.0	34.6	43.0	39.5	49.5	31.8	35.6

The buried volume of phosphinine **1** is very similar to that of PPh_3 (29.2% versus 29.6%).[14] The value for **2** is much higher due to the presence of the sterically demanding $Si(CH_3)_3$ substituents at the α-carbon atoms. As expected, 1-phosphabarrelenes **3** and **5** have larger buried volumes than phosphinine **1** due to their three-dimensional nature compared to the rather flat phosphinine **1** (34.6% and 39.5%, respectively). The $Si(CH_3)_3$-substituted 1-phosphabarrelenes **4** and **6** have even larger buried volumes than extremely bulky phosphines, such as P(*o*-Tol)$_3$ (41.4%) and P(Mes)$_3$ (47.6%).[14] Finally, the values for 5-phosphasemibullvalenes **7** and **8** are

© 2019 Wiley-VCH Verlag GmbH & Co. KGaA, Weinheim

lower than the ones of their precursors **3** and **4**, respectively. In fact, the internal angles are smaller in the fused 5-membered rings of 5-phosphasemibullvalenes and, consequently, the substituents on the α-carbons are pointing away from the metal center compared to 1-phosphabarrelenes.

In order to determine Tolman electronic parameter (TEP, χ) of the phosphorus ligands **1**–**8**, we synthesized the corresponding [(**L**)Ni(CO)$_3$] complexes, which were described for 1-phosphabarrelenes and 5-phosphasemibullvalenes for the first time by our group.[6,11] An excess of [Ni(CO)$_4$] was transferred at −196 °C to a frozen solution of **1**–**8** in tetrahydrofuran in a J-Young NMR tube. Upon thawing of the mixture, a violent gas evolution was detected. The formation of the corresponding [(**L**)Ni(CO)$_3$] complexes was confirmed by ^{31}P{^{1}H} NMR spectroscopy. The reactions were generally fast but in some cases, it was necessary to remove the liberated CO from the NMR tube in order to reach full conversion. Evaporation of the volatiles quantitatively yielded the new coordination compounds as off-white solids. Unfortunately, the Si(CH$_3$)$_3$-substituted phosphinine **2** and the bis(trifluoromethyl)-substituted phosphabarrelene **6** did not react with [Ni(CO)$_4$]. We anticipate that this is due to the close proximity of the sterically demanding Si(CH$_3$)$_3$- and CF$_3$-substituents to the phosphorus atom. In fact, it is known that 2,6-disubstituted Si(CH$_3$)$_3$-phosphinines prefer π-coordination through the aromatic ring towards a metal fragment, rather than σ-coordination.[16] Single crystals of [(**3**)Ni(CO)$_3$] were obtained by slow evaporation of the solvent from a concentrated solution of the coordination compound in THF, the crystal structure of [(**3**)Ni(CO)$_3$] is depicted in Figure 6, along with selected bond lengths and angles. Interestingly, this compound is one of the few crystallographically characterized [(**L**)Ni(CO)$_3$] complexes. Compared to 1-phosphabarrelene **3**, the three P–C bond lengths, as well as the double bonds between C(1) and C(2) in [(**3**)Ni(CO)$_3$] become slightly shorter

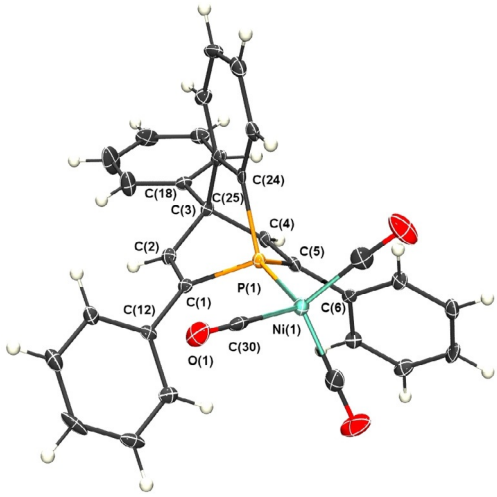

Figure 6. Molecular structure of [(**3**)Ni(CO)$_3$] in the crystal. Displacement ellipsoids are shown at the 50% probability level. Selected bond lengths [Å] and angles [°]: P(1)–C(1) 1.853(3), P(1)–C(5) 1.835(3), P(1)–C(24) 1.829(3), P(1)–Ni(1) 2.1976(8), C(1)–C(2) 1.329(4), C(2)–C(3) 1.533(4), C(3)–C(4) 1.537(4), C(4)–C(5) 1.320(4), C(24)–C(25) 1.401(4), C(25)–C(3) 1.548(4), C(1)-P(1)-C(5) 96.0(1), C(1)-P(1)-C(24) 94.7(1), C(5)-P(1)-C(24) 96.3(1).

upon coordination, which results in a smaller pyramidalization of the phosphorus atom with $\Sigma\measuredangle$(CPC) = 287° with respect to the free ligand **3** ($\Sigma\measuredangle$(CPC) = 283°). The Ni^0 atom displays the expected distorted tetrahedral coordination environment with a P(1)–Ni(1) distance of 2.1976(8) Å.

The corresponding IR spectra of the synthesized [(**L**)Ni(CO)$_3$] complexes were measured in dichloromethane and the experimental values along with the calculated Tolman electronic parameter (χ) are listed in Table 2.

Table 2. Experimental and calculated wavenumbers in [cm^{-1}] for the A$_1$ stretching modes and corresponding Tolman electronic parameter (χ).

Complex	$\tilde{\nu}$(CO)$_{exptl}$	$\tilde{\nu}$(CO)$_{calcd}$	Δ(calcd-exptl)	χ_{exptl}[a]
[(**1**)Ni(CO)$_3$]	2079.2	2080.5	1.3	23.1
[(**2**)Ni(CO)$_3$]	–	2073.6	–	17.5 (calcd)
[(**3**)Ni(CO)$_3$]	2075.0	2075.3	0.3	18.9
[(**4**)Ni(CO)$_3$]	2069.5	2068.5	−1.0	13.4
[(**5**)Ni(CO)$_3$]	2081.2	2080.7	−0.5	25.1
[(**6**)Ni(CO)$_3$]	–	2075.3	–	19.2 (calcd)
[(**7**)Ni(CO)$_3$]	2074.2	2073.4	−0.8	18.1
[(**8**)Ni(CO)$_3$]	2069.0	2068.2	−0.8	12.9

[a] based on $\tilde{\nu}$(CO)$_{exptl}$ = 2056.1 cm^{-1} for P(*t*Bu)$_3$.

Since the χ values for phosphinine **2** and phosphabarrelene **6** could not be identified experimentally, we decided to determine the electronic ligand parameter for all compounds **1**–**8** by means of DFT calculations and to compare the results with the experimental values. The DFT calculations were carried out with Gaussian 09 (Revision D.01[17a]) at the B3PW91/6-31G(d) (LanL2DZ with an additional f-polarization function for Ni) level of theory. For the CO vibration with A$_1$ symmetry a scaling factor of 0.9753 was applied.[17b] Interestingly, the DFT calculations are an excellent approximation of the experimental values, and allowed to assign reliably χ values also for ligands **2** and **6**. Nevertheless, the Tolman electronic parameter reflects only the net-donating ability of a given phosphorus ligand as a separation into σ- and π-contribution is not possible from the IR data. As anticipated, 2,4,6-triphenylphosphinine **1** appears as a very poor net donor with a χ value typical for strongly π-accepting ligands (χ = 23.4 for P(OMe)$_3$).[11c] Phosphinine **2** is a stronger donor as expected for the presence of a β-silyl effect of the Si(CH$_3$)$_3$ groups in α-position to the phosphorus atom.[18] The calculated χ value of 17.5 for **2** suggests that this ligand is a weak donor, with properties similar to the secondary phosphine HPPh$_2$ ($\tilde{\nu}$(CO) = 2073.3 cm^{-1}, χ = 17.2).[11c] From the overall data, it is clear that this trend is similar for the two sets of differently substituted ligands based on **1** and **2**. The electronic properties of the 1-phosphabarrelenes strongly depend on the alkyne that is employed in their synthesis. The benzophosphabarrelenes **3** and **4** show higher net-donation, whereas the bis(trifluoromethyl)-substituted derivatives **5** and **6** are weaker net donors (see Table 2). In fact, **5** is the weakest net donor among the whole series. Finally, the 5-phosphasemibullvalenes **7** and **8** show only slightly higher net-donating properties as the corresponding 1-phosphabarrelene

© 2019 Wiley-VCH Verlag GmbH & Co. KGaA, Weinheim

isomers. It should be noted that the $Si(CH_3)_3$-substituted phosphabarrelene **4** and the $Si(CH_3)_3$-substituted 5-phosphasemibullvalene **8** have χ values of 13.4 and 12.9, respectively and thus, are similar to the good donor PPh_3 ($\tilde{\nu}(CO) = 2068.9\ cm^{-1}$, $\chi = 12.8$).[11c] Figure 7 displays ligands **1**–**8** ordered by increasing net-donation. These values can be compared with the large library that has been compiled by Tolman.

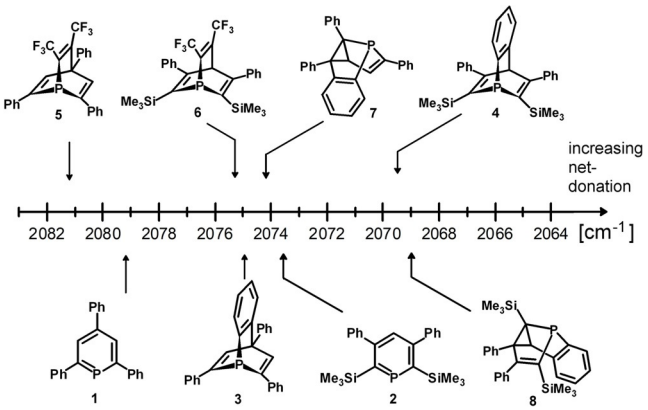

Figure 7. Overview on the experimentally (**1**, **3**–**5**, **7**, **8**) and theoretically (**2**, **6**) determined wavenumbers of the A_1 stretching mode for **1**–**8**.

Additional information can be obtained from further theoretical calculations. In particular, ETS-NOCV is a powerful tool for the quantitative analysis of chemical bonds, combining the extended-transition-state (ETS) method for energy decomposition analysis with the natural orbitals for chemical valence (NOCV) theory.[19] With this method, the energy contributions to the total bond energy are calculated for each specific orbital interaction between the ligand and the metal fragment. In this way, it is possible to decompose the bond into its different components (such as σ, π, δ), providing the corresponding energy contributions to the total bond energy. Calculating the contributions for a set of ligands bound to the same metal fragment allows for a precise comparison of their electronic properties. An extensive overview of the donor and acceptor ability of phosphines obtained by applying ETS-NOCV calculations has recently been reported by Brenna and co-workers.[20]

Also, with respect to applications in gold-catalyzed reactions (vide infra), calculations were performed for [(**L**)AuCl] complexes containing ligands **1**–**8**. The geometry optimizations and ETS-NOCV analyses were performed at the ZORA-PW91/TZ2P level of theory using ADF2016.105 and ADF2016.102, respectively, and the results for σ- and π-contributions in [(**L**)AuCl] type complexes are summarized in Figure 8 (see Supporting Information for details). The L–M distance is an important parameter because it reflects the overlap between the ligand and the metal orbitals, which affects the efficiency of the net-donation. Thus, this can also be influenced by the steric demand of the corresponding ligand.

From the diagrams it is clear that phosphinines are the weakest σ-donors and the strongest π-acceptors. The trimethylsilyl groups in **2** lead to a considerable stronger σ-contribution. The benzophosphabarrelenes **3** and **4** are stronger σ-donors than phosphinines **1** and **2**, but weaker π-acceptors. However, they show smaller σ- and a larger π-contributions than PPh_3. The bis(trifluoromethyl)-substituted phosphabarrelenes **5** and **6** are weaker σ-donors than the benzo-substituted counterparts, yet they are much stronger π-acceptors.

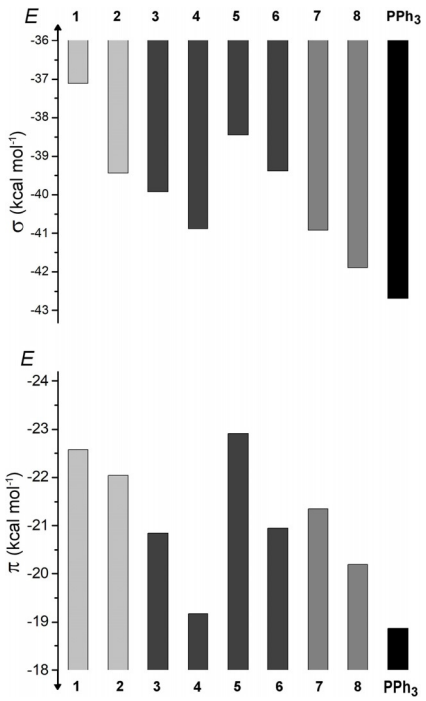

Figure 8. Calculated σ- (top) and π-contribution (bottom) to the L–Au bond in [(**L**)AuCl] type complexes of **1**–**8**, with PPh_3 as a reference. Note the reversed scale of the π-contribution. Different grey shades correspond to different ligand classes: from left to right are reported the values for phosphinines **1** and **2**, benzophosphabarrelenes **3** and **4**, bis(trifluoromethyl)-substituted 1-phosphabarrelenes **5** and **6**, 5-phosphasemibullvalenes **7** and **8**, and PPh_3.

5-Phosphasemibullvalenes **7** and **8** are stronger σ-donors and π-acceptors than the corresponding 1-phosphabarrelenes. Overall, however, they behave as only slightly stronger net-donors. Notably, the selected ligands are weaker σ-donors and stronger π-acceptors than PPh_3. Also, it is evident that the presence of trimethylsilyl groups increases the σ- and decreases the π-contribution, as suggested by the TEP values reported above. This is consistent with the +I effect of the $Si(CH_3)_3$ group, while the negative hyperconjugating effect, which should increase the π-accepting properties, is only marginal. To conclude, phosphinines are strong π-acceptors and weak σ-donors. The properties of the corresponding phosphabarrelenes are dependent on the alkyne that is employed in their synthesis. The electron-poor bis(trifluoromethyl)-substituted phosphabarrelenes are stronger π-acceptors, while benzophosphabarrelenes are stronger σ-donors. The corresponding 5-phosphasemibullvalenes are slightly stronger donors. In general, these ligands have electronic properties, which range among differently substituted phosphites. These results are in line with the molecular orbital scheme of selected compounds. Figure 9 shows a graphical representation of the relevant frontier orbitals of **1**, **3**, **5** and **7**.

© 2019 Wiley-VCH Verlag GmbH & Co. KGaA, Weinheim

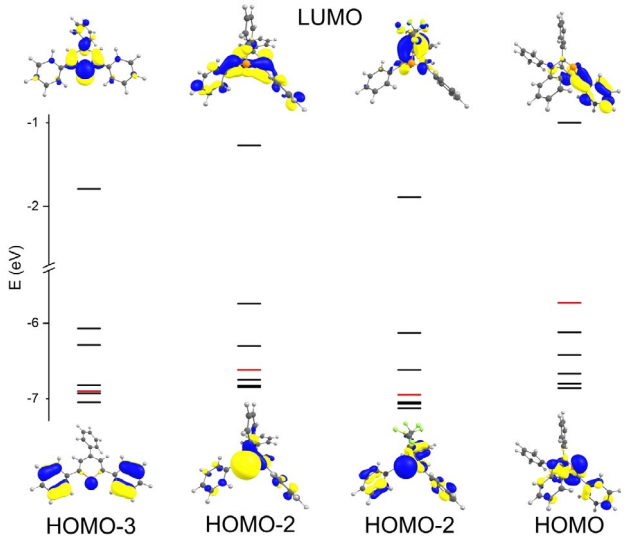

Figure 9. Molecular orbital (MO) scheme for **1**, **3**, **5**, **7** (from left to right). Orbitals from LUMO to HOMO−3 are shown. The molecular orbital, which represents the lone pair, is depicted in red.

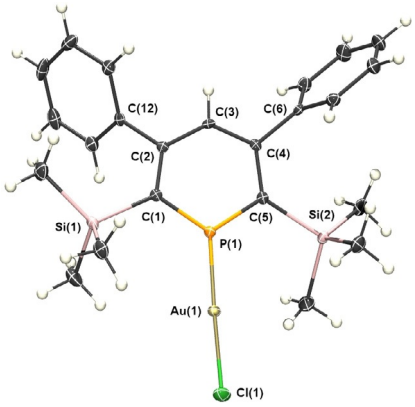

Figure 10. Molecular structure of [(**2**)AuCl] in the crystal. Displacement ellipsoids are shown at the 50% probability level. Selected bond lengths [Å] and angles [°]: P(1)–C(1) 1.722(3), P(1)–C(5) 1.721(3), P(1)–Au(1) 2.2083(7), Au(1)–Cl(1) 2.2707(7), C(1)–C(2) 1.410(4), C(2)–C(3) 1.399(4), C(3)–C(4) 1.401(4), C(4)–C(5) 1.411(4), C(1)–Si(1) 1.914(3), C(5)–Si(2) 1.915(3), C(1)-P(1)-C(5) 112.0(1), P(1)-Au(1)-Cl(1), 176.82(3).

The lone pair of 2,4,6-triphenylphosphinine **1** is essentially represented by the energetically low-lying HOMO−3. **5** has similar σ-donor properties, while **3** and **7** are the strongest σ-donors of the series. The trend is confirmed also for the LUMO orbitals. Phosphinine **1** and bis(trifluoromethyl)-substituted 1-phosphabarrelene **5** have strong π-acceptor properties, while the energy level of their lowest unoccupied molecular orbitals is similar and low in energy. 1-Phosphabarrelene **3** and 5-phosphasemibullvalene **7** are weaker π-acceptors, therefore the LUMO orbitals are located higher in energy. As expected for phosphine derivatives, the LUMOs of phosphabarrelenes and phosphasemibullvalenes correspond to σ*-orbitals of the P–C bonds, whereas it is of π-symmetry for the phosphinine.

Before we started to investigate the application of **1**–**8** as ligands in gold-catalyzed reactions, we explored their coordination chemistry towards Au^I. According to $^{31}P\{^1H\}$ NMR spectroscopy, all these phosphorus compounds react quantitatively with $[AuCl(SMe_2)]$ in dichloromethane to form the corresponding Au^I complexes [(**L**)AuCl]. This is particularly important for phosphinine **2**, as the sterically demanding $Si(CH_3)_3$ groups could prevent σ-coordination to a metal fragment, although it is not the case for [(**2**)AuCl]. All coordination compounds were obtained as off-white solids after removal of the solvent and all the volatiles. Single crystals of [(**2**)AuCl], suitable for X-ray diffraction, were obtained by slow evaporation of solvent from a concentrated solution of [(**2**)AuCl] in dichloromethane at −35 °C. The molecular structure of this compound in the crystal, along with selected bond lengths and angles, is depicted in Figure 10.

As also observed for the few crystallographically characterized phosphinine-Au^I complexes, the metal center in [(**2**)AuCl] is coordinated in a nearly linear fashion with a P-Au-Cl angle of 176.82(3)° and a P(1)–Au(1) bond length of 2.2083(7) Å. Interestingly, as observed also for a related Au^I complex, the internal C(1)-P(1)-C(5) angle is surprisingly large compared to 2,4,6-triaryl-substituted phosphinine metal complexes (112° versus 106°).[21] This can be attributed to the large steric demand of the $Si(CH_3)_3$ groups at the α-carbons. A closer look to the packing of [(**2**)AuCl] in the crystal lattice shows no aurophilic interactions between neighboring molecules.

We were also able to characterize [(**3**)AuCl] and [(**4**)AuCl] crystallographically. Single crystals, suitable for X-ray diffraction, were again obtained by slow evaporation of the solvent from concentrated solutions of the coordination compounds in dichloromethane at −35 °C. The molecular structures of [(**3**)AuCl] and [(**4**)AuCl] in the crystal, along with selected bond lengths and angles, are depicted in Figures 11 and 12, respectively. As

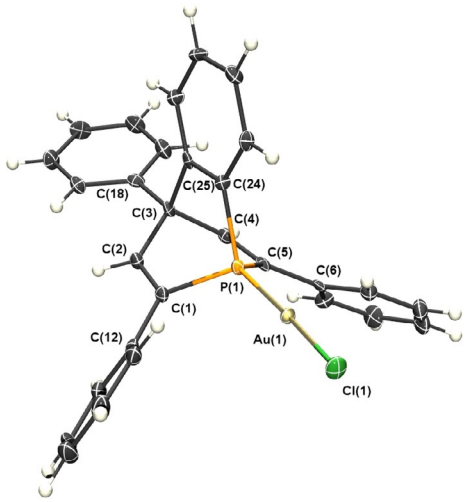

Figure 11. Molecular structure of [(**3**)AuCl] in the crystal. Displacement ellipsoids are shown at the 50% probability level. Only one independent molecule is shown. Selected bond lengths [Å] and angles [°]: P(1)–C(1) 1.829(4), P(1)–C(5) 1.840(4), P(1)–C(24) 1.815(4), P(1)–Au(1) 2.216(1), Au(1)–Cl(1) 2.283(1), C(1)–C(2) 1.333(6), C(2)–C(3) 1.525(5), C(3)–C(4) 1.540(6), C(4)–C(5) 1.331(6), C(24)–C(25) 1.403(6), C(25)–C(3) 1.551(6), C(1)-P(1)-C(5) 99.1(2), C(1)-P(1)-C(24) 98.3(2), C(5)-P(1)-C(24) 95.9(2), P(1)-Au(1)-Cl(1) 174.79(4).

© 2019 Wiley-VCH Verlag GmbH & Co. KGaA, Weinheim

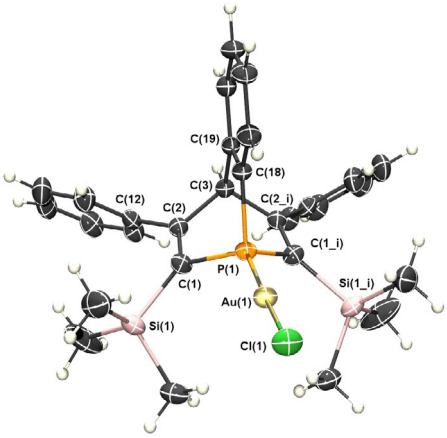

Figure 12. Molecular structure of [(**4**)AuCl] in the crystal. Displacement ellipsoids are shown at the 50% probability level. Selected bond lengths [Å] and angles [°]: P(1)–C(1) 1.836(4), P(1)–C(18) 1.817(5), P(1)–Au(1) 2.2286(13), Au(1)–Cl(1) 2.2827(13), Si(1)–C(1) 1.889(4), C(1)–C(2) 1.347(5), C(2)–C(3) 1.535(5), C(18)–C(19) 1.399(8), C(19)–C(3) 1.533(7), C(1)-P(1)-C(1_i) 100.8(2), C(1)-P(1)-C(18) 99.10(17), P(1)-Au(1)-Cl(1) 175.98(5).

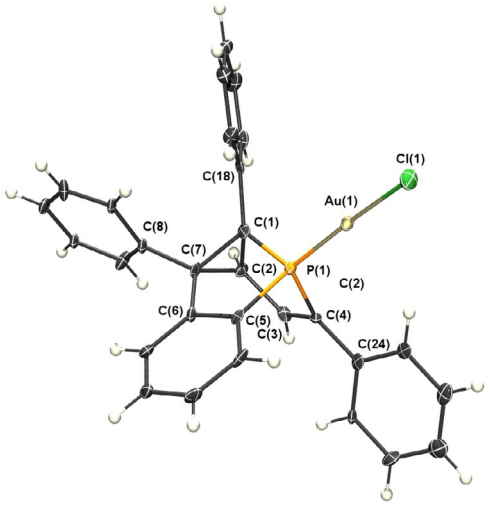

Figure 13. Molecular structure of [(**7**)AuCl] in the crystal. Displacement ellipsoids are shown at the 50% probability level. Only one enantiomer is shown. Selected bond lengths [Å] and angles [°]: P(1)–C(1) 1.853(12), P(1)–C(4) 1.827(11), P(1)–C(5) 1.795(12), P(1)–Au(1) 2.211(3), Au(1)–Cl(1) 2.277(3), C(1)–C(2) 1.508(15), C(1)–C(7) 1.522(15), C(2)–C(7) 1.558(15), C(2)–C(3) 1.514(16), C(3)–C(4) 1.331(16), C(5)–C(6) 1.410(15), C(6)–C(7) 1.492(15), C(1)-P(1)-C(5) 94.1(5), C(1)-P(1)-C(4) 94.5(5), C(4)-P(1)-C(5) 95.8(5), P(1)-Au(1)-Cl(1) 176.11(11).

both **3** and **4** have been characterized by means of X-ray diffraction, structural changes upon coordination of the ligands to the [AuCl] fragment can be discussed. In [(**3**)AuCl], the three P–C bond lengths are by approximately 0.02 Å shorter compared to uncomplexed **3**, while all C–C bond lengths within the [2.2.2]-bicycle are very similar for both [(**3**)AuCl] and **3**. Therefore, a significant smaller pyramidalization of the phosphorus atom with $\Sigma\measuredangle$(CPC) = 293.3° with respect to the free ligand **3** ($\Sigma\measuredangle$(CPC) = 283°) is observed. The Au(1) atom displays the expected linear coordination environment with a P(1)-Au(1)-Cl(1) angle of 174.79(4)° and a P(1)–Au(1) interatomic distance of 2.216(1) Å.

A similar situation is observed when comparing **4** with [(**4**)AuCl]. The three P–C bond lengths in the coordination compound are approximately 0.03 Å shorter than in the free ligand, while the C–C interatomic distances in both [2.2.2]-bicycles are very similar. This results in a pyramidalization of the phosphorus atom of $\Sigma\measuredangle$(CPC) = 300.7° compared to $\Sigma\measuredangle$(CPC) = 286.9° in the free ligand. Again, an almost linear coordination environment for the gold atom is observed (P(1)-Au(1)-Cl(1) = 175.98(5)°). The P(1)–Au(1) bond length of 2.2286(13) Å is slightly longer than in [(**3**)AuCl].

Finally, we could also obtain single crystals suitable for X-ray diffraction of the Au^I complex containing the 5-phosphasemibullvalene **7**, as the first example of a crystallographically characterized 5-phosphasemibullvalene metal complex (Figure 13). As the photochemical di-π-methane rearrangement of **3** to **7** produces a mixture of enantiomers of **7**, [(**7**)AuCl] exists as a racemate in the asymmetric unit. The P(1)–Au(1) bond length is with 2.211(3) Å shorter than in [(**3**)AuCl] (2.216(1)).

During the last two decades, homogeneous gold-catalyzed reactions underwent a major development.[22] The reactivity of Au^I species towards unsaturated C–C bonds, which for a long time was neglected, is the main focus of a large number of reviews.[23] These reports mostly deal with reactions where an electrophilic, usually cationic, gold center activates a C–C multiple bond by coordination, allowing a nucleophilic attack on the otherwise unreactive substrate. The cationic gold species is usually formed from the corresponding [(**L**)AuCl] type complex and a chloride scavenger, such as a silver salt. This approach has been extended to intramolecular reactions, such as cycloisomerizations.[23,24]

In these reactions the choice of the ancillary ligands is crucial, as the putative cationic gold species usually needs to be stabilized by relatively bulky and strong donor ligands, such as phosphines or carbenes.[23c,25] However, strong π-accepting phosphites in combination with Au^I precursors often show remarkable catalytic activities in such reactions, but these systems sometimes suffer from their instability.[26] So far, none of the new ligands described in this work, except for **1**, have ever been employed in a gold-catalyzed homogeneous transformation.[4e] Since their electronic properties have been carefully evaluated and span across a large range of phosphites, it is interesting to test them in these reactions.

A typical benchmark reaction in homogeneous Au^I catalysis is the cycloisomerization of the 1,6-enyne dimethyl 2-(3-methylbut-2-enyl)-2-(prop-2-ynyl)malonate towards the corresponding cyclopentene-derivative.[24] Several phosphorus-containing ligands have been employed in this metal-mediated transformation.[27] Yoshifuji and Ito have successfully applied also phosphaalkenes as ligands, even without any additive.[28] Apparently, the highly π-accepting properties of phosphaalkenes are beneficial for increasing the Lewis acidity of the gold centers. In a comparison study with a structurally related mesoionic carbene, we recently investigated the use of phosphinine-based Au^I complexes as precatalysts in the cycloisomerization of dimethyl 2-(3-methylbut-2-enyl)-2-(prop-2-ynyl)malonate and *N*-2-propyn-1-ylbenzamide (**9**), respectively (Scheme 1).

© 2019 Wiley-VCH Verlag GmbH & Co. KGaA, Weinheim

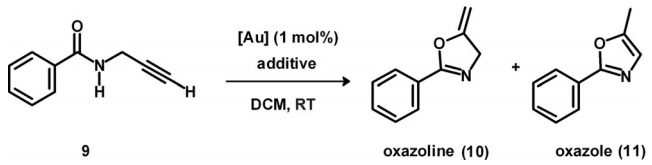

Scheme 1. Cycloisomerization of *N*-2-propyn-1-ylbenzamide (**9**) towards oxazoline (**10**) and oxazole (**11**).

We found that the phosphinine-based catalytic system is more active and selective than the mesoionic carbene-based one, particularly in the transformation of the more challenging substrate **9**.[4e] These results demonstrated for the first time, that particularly sterically demanding 2,4,6-triarylphosphinine-derivatives can be used efficiently as π-accepting ligands in Au^I-catalyzed homogenous transformations. Therefore, we decided to compare phosphinines, 1-phosphabarrelenes and phosphasemibullvalenes **1**–**8** in the Au^I-catalyzed cycloisomerization of **9**, which is more difficult to convert than the standard reagent dimethyl 2-(3-methylbut-2-enyl)-2-(prop-2-ynyl)-malonate.

We first evaluated the reactivity of phosphinine-gold complexes towards **9**.[29] It is well established that the P=C bond in phosphinine-based coordination compounds can react irreversibly with protic reagents, such as amines, alcohols and water.[30] This would lead to a modified catalytic system. Even though amides are very weak acids, the N–H functionality of the substrate could undergo a formal addition to the P=C double bond of the phosphinine ligands. To exclude this possibility, an equivalent of the substrate was added to [(**L**)AuCl] complex (L = **1** or **2**) and the resulting mixture was stirred in dichloromethane at room temperature. As expected, the $^{31}P\{^1H\}$ NMR spectrum did not show any reaction between the substrate and the coordinated ligand, even after 16 h.

Next, the reactivity of the substrate **9** towards either $AgSbF_6$ or the Au^I precursor [AuCl(SMe$_2$)] was investigated and no conversion was detected (Table 3, entries 1 and 2). Combination of [AuCl(SMe$_2$)] and $AgSbF_6$ led to a high conversion, but the reaction was rather slow (24 h) and unselective (entry 3). In the absence of any silver salt, the neutral [(**L**)AuCl] complexes containing phosphinines **1** and **2** showed only low catalytic activity in the cycloisomerization reaction (entries 4 and 6). However, a clear contrast between the two phosphinine-based complexes was observed in the presence of the chloride scavenger, which indicates the presence of the putative $[(\mathbf{L})Au]^+$ species. In combination with $AgSbF_6$, a very active catalytic species was formed using **2** as ligand, and a high conversion and a good selectivity towards the oxazoline **10** (9:1) was achieved after 6 h (entry 7). On the other hand, the catalyst based on phosphinine **1** was less active and gave 40% of a mixture of products within 24 h (entry 5). Interestingly, both catalytic activities and selectivities of [AuCl(PPh$_3$)]/$AgSbF_6$ and [(P(OR)$_3$AuCl]/$AgSbF_6$ (P(OR)$_3$ = tris(2,4-di-*tert*-butylphenyl)phosphite) were very similar, whereas the catalyst based on **2** outperformed these systems (entries 8 and 9 versus entry 7).

At this point, the evaluation of the electronic properties reported above can help to shed light on the obtained results. It is reasonable to assume that 2,4,6-triphenylphosphinine (**1**) forms a kinetically less stable Au^I complex compared to ligand **2**, most likely due to a combination of steric and electronic effects (29.2% V_{bur} versus 38.0% V_{bur}). The ETS-NOCV analysis suggests that phosphinine **2**, as a considerably stronger σ-donor, stabilizes the putative catalytically active cationic gold species better than **1**.

Neither 1-phosphabarrelenes, nor 5-phosphasemibullvalenes have so far been applied as ligands in homogeneous Au^I-catalyzed reactions. Table 4 shows the results of the cycloisomerization of **9** with 1-phosphabarrelenes **3**–**6** as ligands. In the absence of $AgSbF_6$, the 1-phosphabarrelenes **3** and **5**, based on phosphinine **1**, led to a low catalytic activity of the corresponding catalyst, while the 1-phosphabarrelenes **4** and **6**, based on phosphinine **2**, formed inactive catalysts (entries 1 and 5 versus entries 3 and 7). On the other hand, a much higher activity for all the Au^I complexes was observed in the presence of the silver salt. Catalysts based on benzophosphabarrelenes **3** and **4** performed similarly and reached full conversion within 2.5 h with a substrate selectively of 100% towards oxazoline **10** (entries 2 and 4). Likewise, trifluoromethyl-substituted derivatives **5** and **6** formed active species that showed very high conversions (96% and >99%, respectively, entries 6 and 8) and a high selectivity towards oxazoline **10**, even though the substrate took longer to be fully converted. The longer reac-

Table 3. Catalytic cycloisomerization of substrate **9** to oxazoline (**10**) and oxazole (**11**). Conditions: catalyst precursor: 1 mol%, chloride scavenger: 1 mol% $AgSbF_6$, dichloromethane, room temperature.

Entry	Precatalyst	Additive	Time [h]	Conv [%]	Product ratio **10**:**11**
1	–	$AgSbF_6$	24	0	–
2	[AuCl(SMe$_2$)]	–	24	0	–
3	[AuCl(SMe$_2$)]	$AgSbF_6$	24	85	9:1
4	[(**1**)AuCl]	–	24	25	0:1
5	[(**1**)AuCl]	$AgSbF_6$	24	40	4:1
6	[(**2**)AuCl]	–	24	40	9:1
7	[(**2**)AuCl]	$AgSbF_6$	6	>99	9:1
8	[(PPh$_3$)AuCl]	$AgSbF_6$	7	>99	96:4
9	[(P(OR)$_3$)AuCl][a]	$AgSbF_6$	11	>99	98:2

[a] P(OR)$_3$ = tris(2,4-di-*tert*-butylphenyl)phosphite.

Table 4. Results for the catalytic cycloisomerization of substrate **9** to **10** and **11**. Conditions: catalyst precursor: 1 mol%, chloride scavenger: 1 mol% $AgSbF_6$, dichloromethane, room temperature.

Entry	Precatalyst	Additive	Time [h]	Conv [%]	Product ratio **10**:**11**
1	[(**3**)AuCl]	–	24	50	92:8
2	[(**3**)AuCl]	$AgSbF_6$	2.5	>99	1:0
3	[(**4**)AuCl]	–	24	0	0
4	[(**4**)AuCl]	$AgSbF_6$	2.5	>99	1:0
5	[(**5**)AuCl]	–	24	65	3:1
6	[(**5**)AuCl]	$AgSbF_6$	6	96	98:2
7	[(**6**)AuCl]	–	24	0	0
8	[(**6**)AuCl]	$AgSbF_6$	5	>99	1:0

© 2019 Wiley-VCH Verlag GmbH & Co. KGaA, Weinheim

tion time could be due to the weaker σ-donation of these ligands, which is comparable to that of phosphinines. Interestingly, the comparison between benzophosphabarrelene **3** and trifluoromethyl-derivative **6** shows that even though the electronic properties of these ligands are almost identical, a rather different reactivity is observed (full conversion in 2.5 h versus 5 h). This can only be attributed to the considerably different steric bulk of the two ligands, which is extremely large for **6** (34.6 %V_{bur} versus 49.5 %V_{bur}).

Finally, the 5-phosphasemibullvalenes **7** and **8** were investigated in the Au^I-catalyzed cycloisomerization of **9** and the results are summarized in Table 5. Au^I-catalysts based on **7** and **8** reacted in a similar way as the corresponding benzobarrelenes **3** and **4**. Full conversion of the substrate exclusively to **10** with only slightly longer reaction times were observed (3 h versus 2.5 h, entries 2 and 4). As already mentioned, considerable differences in the electronic properties exist especially between aryl- and $Si(CH_3)_3$-substituted derivatives. In fact, the latter ones are both stronger σ-donors and weaker π-acceptors than the aryl-substituted counterparts. This results in a higher net-donation, as observed for the χ values of the corresponding [(**L**)Ni(CO)$_3$] complexes (vide supra). The difference in the catalytic activity seems to correlate with the steric bulk of the ligands, which is lower for 5-phosphasemibullvalenes (34.6 %V_{bur} and 43.0 %V_{bur} versus 31.8 %V_{bur} and 35.6 %V_{bur}). In fact, this could lead to less kinetically stable gold complexes.

Table 5. Results for the catalytic cycloisomerization of substrate **9** to **10** and **11**. Conditions: catalyst precursor: 1 mol%, chloride scavenger: 1 mol% $AgSbF_6$, dichloromethane, room temperature.

Entry	Precatalyst	Additive	Time [h]	Conv [%]	Product ratio **10**:**11**
1	[(**7**)AuCl]	–	24	0	–
2	[(**7**)AuCl]	$AgSbF_6$	3	>99	1:0
3	[(**8**)AuCl]	–	24	62	98:2
4	[(**8**)AuCl]	$AgSbF_6$	3	>99	1:0

The reactivity of cationic Au^I species is usually considered to strongly correlate with the stabilization of cationic intermediates by means of π-back-bonding from the gold atom.[31] However, some theoretical studies state that this contribution has only a marginal effect.[32] The results presented here suggest that the σ-donor properties of the ancillary ligands are the most important contribution for the achievement of a kinetically stable catalytic species. On the other hand, the large difference in the π-back-donation properties of the selected ligands is not reflected by the catalytic activity. This data suggest that the π-accepting properties of the ligand have a secondary role in this reaction, while the σ-donation and the steric bulk seem to be the most important parameters. A complex interplay between these two characteristics appears to be the key to a successful stabilization of the catalytic species. In this respect, bulky benzophosphabarrelene and related 5-phosphasemibullvalenes are good candidates for this reaction.

Finally, a time-conversion plot for the cycloisomerization of **9** with the best performing catalytic systems in terms of activity and selectivity ([(**3**)AuCl]/$AgSbF_6$ and [(**7**)AuCl]/$AgSbF_6$) allows a direct comparison with Au^I catalysts based on classical ligands, such as PPh_3 and $P(OR)_3$ (tris(2,4-di-*tert*-butylphenyl)-phosphite). The conversion of the substrate was determined by means of ^{1}H NMR spectroscopy during specific time intervals (Figure 14). From Figure 14 is it possible to extrapolate the turnover frequencies (TOF) values for these catalysts at 20 % conversion (Table 6). These values show that the activity of the catalytic systems described in this work is comparable with the reported data of state-of-the-art cationic phosphorus-based gold catalysts used for this particular substrate.[29d,g,33] Interestingly, the highest value is observed for the catalytic system based on the novel 5-phosphasemibullvalene **7** (TOF = 104 h^{-1}).

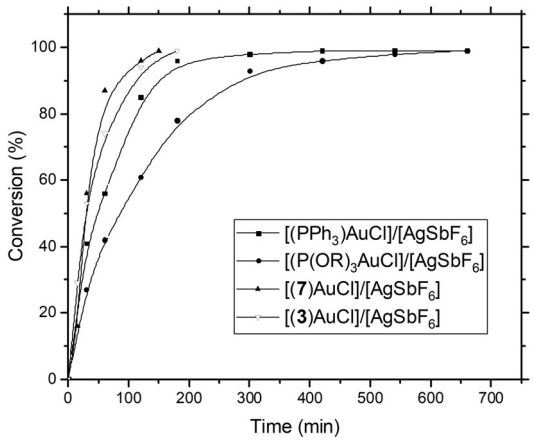

Figure 14. Conversion versus time plot for the catalytic systems based on 1-phosphabarrelene **3** and 5-phosphasemibullvalene **7**, as well as PPh_3 and $P(OR)_3$ (tris(2,4-di-*tert*-butylphenyl)phosphite) as reference catalysts.

Table 6. TOF values for the catalytic systems based on **3**, **7**, and the reference catalysts.

Ligand	Catalyst	TOF [h^{-1}]
3	[(**3**)AuCl]/[$AgSbF_6$]	98
7	[(**7**)AuCl]/[$AgSbF_6$]	104
PPh_3	[(PPh_3)AuCl]/[$AgSbF_6$]	91
$P(OR)_3$[a]	[($P(OR)_3$)AuCl]/[$AgSbF_6$]	49

[a] $P(OR)_3$ = tris(2,4-di-*tert*-butylphenyl)phosphite.

Conclusions

The steric and electronic properties of the related phosphinines, 1-phosphabarrelenes and 5-phosphasemibullvalenes with respect to potential applications as phosphorus ligands in homogeneous catalysis have been thoroughly evaluated. The steric properties of these compounds have been determined by calculating their buried volume (%V_{bur}). In the case of phosphinines, the steric bulk is related to the substituents on the α-carbon atoms. The corresponding 1-phosphabarrelenes are

© 2019 Wiley-VCH Verlag GmbH & Co. KGaA, Weinheim

remarkably bulky, trifluoromethyl-substituted derivatives having the highest %V_{bur}. In contrast, 5-phosphasemibullvalenes are less sterically demanding. The electronic properties of the ligands have been evaluated both theoretically and experimentally. The Tolman electronic parameter was measured or calculated for all the ligands, which provides a detailed comparison of the net-donation properties of the three classes of ligands. Trifluoromethyl-substituted phosphabarrelenes are the weakest net donors, followed by phosphinines. The net-donation of phosphabarrelenes and phosphasemibullvalenes is higher and very similar, making them the strongest donors among the ligands of this work. ETS-NOCV calculations on [(**L**)AuCl] complexes allowed the evaluation of the single σ- and π-contributions to the L–M bond, thus giving a deeper insight into their electronic properties. Moreover, new Au^{I} complexes bearing phosphinines, 1-phosphabarrelenes and 5-phosphasemibullvalenes as ligands have been characterized. In combination with Au^{I}, most of these ligands quantitatively and selectively performed the cycloisomerization of *N*-2-propyn-1-ylbenzamide towards its oxazoline constitutional isomer in a short time. The results are comparable to the best catalytic systems found in the literature. Although the strong π-accepting properties of these ligands could be beneficial for the formation of strongly electrophilic Au^{+} centers, these properties seem to have a minor role for the successful conversion of propargyl amides. The stabilization of the catalytic species appears to benefit from a relatively strong donation and large steric bulk.

Experimental Section

CCDC 1896131, 1896132, 1896133, 1896134, 1896135, 1896136, 1896137 and 1896138 contain the supplementary crystallographic data for this paper. These data can be obtained free of charge from The Cambridge Crystallographic Data Centre.

Acknowledgements

Financial support was provided by the European Initial Training Network SusPhos (317404), Freie Universität Berlin, the Deutsche Forschungsgemeinschaft (DFG) and Council for Chemical Sciences of The Netherlands Organization for Scientific Research (NWO/CW) by a VIDI grant (J.C.S.). Tetiana Krachko is kindly acknowledged for the calculations reported in Figure 9. Julian Sklorz is gratefully acknowledged for the crystallographic characterization of [(**3**)Ni(CO)$_3$]. Chady Irigo is kindly acknowledged for fruitful discussions.

Conflict of interest

The authors declare no conflict of interest.

Keywords: density functional calculations · heterocycles · homogeneous gold catalysis · phosphorus ligands · X-ray diffraction

[1] a) G. Märkl, *Angew. Chem.* **1966**, *78*, 907; b) A. J. Ashe III, *J. Am. Chem. Soc.* **1971**, *93*, 3293.
[2] For recent Reviews see: a) P. Le Floch, *Coord. Chem. Rev.* **2006**, *250*, 627; b) F. Mathey, *Angew. Chem. Int. Ed.* **2003**, *42*, 1578; *Angew. Chem.* **2003**, *115*, 1616; c) P. Le Floch, F. Mathey, *Coord. Chem. Rev.* **1998**, *178–180*, 771; d) N. Mézailles, F. Mathey, P. Le Floch in *Progress in Inorganic Chemistry, Vol. 49* (Ed.: K. D. Karlin), Wiley, New York, **2001**, p. 455; e) L. Weber, *Angew. Chem. Int. Ed.* **2002**, *41*, 563; *Angew. Chem.* **2002**, *114*, 583; f) F. Mathey, P. Le Floch, in *Science of Synthesis, Vol 5* (Ed.: M. Moloney), Thieme Chemistry, **2005**, p. 1097; g) C. Müller, D. Vogt, *Dalton Trans.* **2007**, 5505; h) L. Kollár, G. Keglevich, *Chem. Rev.* **2010**, *110*, 4257; i) C. Müller, D. Vogt, *C. R. Chimie* **2010**, *13*, 1127; j) C. Müller, D. Vogt in *Catalysis and Material Science Applications, Vol. 36* (Eds.: M. Peruzzini, L. Gonsalvi), Springer, Berlin, **2011**, Chap. 6; k) C. Müller in *Phosphorus Ligand Effects in Homogeneous Catalysis: Design and Synthesis* (Eds.: P. C. J. Kamer, P. W. N. M. van Leeuwen), Wiley-VCH, Weinheim, **2012**; l) C. Müller, L. E. E. Broeckx, I. de Krom, J. J. M. Weemers, *Eur. J. Inorg. Chem.* **2013**, 187; m) C. Müller, J. A. W. Sklorz, I. de Krom, A. Loibl, M. Habicht, M. Bruce, G. Pfeifer, J. Wiecko, *Chem. Lett.* **2014**, *43*, 1390; n) C. Müller, *Eur. J. Inorg. Chem.* **2016**, 569.
[3] F. Knoch, F. Kremer, U. Schmidt, U. Zenneck, P. Le Floch, F. Mathey, *Organometallics* **1996**, *15*, 2713.
[4] a) J. J. M. Weemers, W. N. P. van der Graaff, E. A. Pidko, M. Lutz, C. Müller, *Chem. Eur. J.* **2013**, *19*, 8991; b) S. Aguado-Ullate, J. A. Baker, V. González-González, C. Müller, J. D. Hirst, J. J. Carbó, *Catal. Sci. Technol.* **2014**, *4*, 979; c) L. E. E. Broeckx, A. Bucci, C. Zuccaccia, M. Lutz, A. Macchioni, C. Müller, *Organometallics* **2015**, *34*, 2943; d) N. Fey, S. Papadouli, P. G. Pringle, A. Ficks, J. T. Fleming, L. J. Higham, J. F. Wallis, D. Carmichael, N. Mézailles, C. Müller, *Phosphorus Sulfur Silicon Relat. Elem.* **2015**, *190*, 706; e) M. Rigo, L. Hettmanczyk, F. J. L. Heutz, S. Hohloch, M. Lutz, B. Sarkar, C. Müller, *Dalton Trans.* **2017**, *46*, 86; f) R. J. Newland, M. F. Wyatt, R. L. Wingad, S. M. Mansell, *Dalton Trans.* **2017**, *46*, 6172; g) R. J. Newland, J. M. Lynam, S. M. Mansell, *Chem. Commun.* **2018**, *54*, 5482; h) R. J. Newland, A. Smith, D. M. Smith, N. Fey, M. J. Hanton, S. M. Mansell, *Organometallics* **2018**, *37*, 1062; i) R. J. Newland, M. P. Delve, R. Wingad, S. M. Mansell, *New J. Chem.* **2018**, *42*, 19625.
[5] a) G. Märkl, F. Lieb, *Angew. Chem. Int. Ed. Engl.* **1968**, *7*, 733; *Angew. Chem.* **1968**, *80*, 702; b) G. Märkl, F. Lieb, C. Martin, *Tetrahedron Lett.* **1971**, *12*, 1249; c) G. Märkl, K. H. Heier, *Tetrahedron Lett.* **1974**, *15*, 4369; d) S. Welfelé, N. Mézailles, N. Maigrot, L. Ricard, F. Mathey, P. Le Floch, *New J. Chem.* **2001**, *25*, 1264; e) A. Moores, L. Ricard, P. Le Floch, *Angew. Chem. Int. Ed.* **2003**, *42*, 4940; *Angew. Chem.* **2003**, *115*, 5090; f) O. Piechaczyk, M. Doux, L. Ricard, P. Le Floch, *Organometallics* **2005**, *24*, 1204; g) E. Fuchs, M. Keller, B. Breit, *Chem. Eur. J.* **2006**, *12*, 6930; h) B. Breit, E. Fuchs, *Synthesis* **2006**, 2121; i) A. Moores, T. Cantat, L. Ricard, N. Mézailles, P. Le Floch, *New J. Chem.* **2007**, *31*, 1493; j) C. Müller, E. A. Pidko, D. Totev, M. Lutz, A. L. Spek, R. A. van Santen, D. Vogt, *Dalton Trans.* **2007**, 5372; k) M. Blug, C. Guibert, X.-F. Le Goff, N. Mézailles, P. Le Floch, *Chem. Commun.* **2008**, DOI: 10.1039/B814886D; l) C. Wallis, P. G. Edwards, M. Hanton, P. D. Newman, A. Stasch, C. Jones, R. P. Tooze, *Dalton Trans.* **2009**, 2170; m) P. S. Bäuerlein, I. A. Gonzalez, J. J. M. Weemers, M. Lutz, A. L. Spek, D. Vogt, C. Müller, *Chem. Commun.* **2009**, 4944; n) M. Blug, X.-F. Le Goff, N. Mézailles, P. Le Floch, *Organometallics* **2009**, *28*, 2360; o) P. Ribagnac, M. Blug, J. Villa-Uribe, X.-F. Le Goff, C. Gosmini, N. Mézailles, *Chem. Eur. J.* **2011**, *17*, 14389; p) D. Ortiz, M. Blug, X.-F. Le Goff, P. Le Floch, N. Mézailles, P. Maître, *Organometallics* **2012**, *31*, 5975; q) M. Rigo, J. A. W. Sklorz, N. Hatje, F. Noack, M. Weber, J. Wiecko, C. Müller, *Dalton Trans.* **2016**, *45*, 2218.
[6] M. Rigo, M. Weber, C. Müller, *Chem. Commun.* **2016**, *52*, 7090.
[7] N. Avarvari, P. Le Floch, F. Mathey, *J. Am. Chem. Soc.* **1996**, *118*, 11978.
[8] For the photochemical di-π-methane rearrangement of CF_3-substituted barrelenes see also: R. S. Liu, *J. Am. Chem. Soc.* **1968**, *90*, 215.
[9] a) A. G. Orpen, N. G. Connelly, *Organometallics* **1990**, *9*, 1206; b) B. J. Dunne, R. B. Morris, A. G. Orpen, *J. Chem. Soc. Dalton Trans.* **1991**, 653.
[10] D. W. Allen, B. F. Taylor, *J. Chem. Soc. Dalton Trans.* **1982**, 51.
[11] a) C. A. Tolman, *J. Am. Chem. Soc.* **1970**, *92*, 2956; b) C. A. Tolman, W. C. Seidel, L. W. Gosser, *J. Am. Chem. Soc.* **1974**, *96*, 53; c) C. A. Tolman, *Chem. Rev.* **1977**, *77*, 313.
[12] E. F. DiMauro, M. C. Kozlowski, *J. Chem. Soc. Perkin Trans. 1* **2002**, 439.

© 2019 Wiley-VCH Verlag GmbH & Co. KGaA, Weinheim

[13] a) L. Cavallo, A. Correa, C. Costabile, H. Jacobsen, *J. Organomet. Chem.* **2005**, *690*, 5407; b) A. Poater, F. Ragone, S. Giudice, C. Costabile, R. Dorta, S. P. Nolan, L. Cavallo, *Organometallics* **2008**, *27*, 2679.
[14] H. Clavier, S. P. Nolan, *Chem. Commun.* **2010**, *46*, 841.
[15] a) A. Poater, B. Cosenza, A. Correa, S. Giudice, F. Ragone, V. Scarano, L. Cavallo, *Eur. J. Inorg. Chem.* **2009**, 1759; b) L. Falivene, R. Credendino, A. Poater, A. Petta, L. Serra, R. Oliva, V. Scarano, L. Cavallo, *Organometallics* **2016**, *35*, 2286.
[16] M. Doux, L. Ricard, F. Mathey, P. Le Floch, N. Mézailles, *Eur. J. Inorg. Chem.* **2003**, 687.
[17] a) Gaussian 09, Revision D.01, M. J. Frisch, G. W. Trucks, H. B. Schlegel, G. E. Scuseria, M. A. Robb, J. R. Cheeseman, G. Scalmani, V. Barone, B. Mennucci, G. A. Petersson, H. Nakatsuji, M. Caricato, X. Li, H. P. Hratchian, A. F. Izmaylov, J. Bloino, G. Zheng, J. L. Sonnenberg, M. Hada, M. Ehara, K. Toyota, R. Fukuda, J. Hasegawa, M. Ishida, T. Nakajima, Y. Honda, O. Kitao, H. Nakai, T. Vreven, J. A. Montgomery, Jr., J. E. Peralta, F. Ogliaro, M. Bearpark, J. J. Heyd, E. Brothers, K. N. Kudin, V. N. Staroverov, R. Kobayashi, J. Normand, K. Raghavachari, A. Rendell, J. C. Burant, S. S. Iyengar, J. Tomasi, M. Cossi, N. Rega, J. M. Millam, M. Klene, J. E. Knox, J. B. Cross, V. Bakken, C. Adamo, J. Jaramillo, R. Gomperts, R. E. Stratmann, O. Yazyev, A. J. Austin, R. Cammi, C. Pomelli, J. W. Ochterski, R. L. Martin, K. Morokuma, V. G. Zakrzewski, G. A. Voth, P. Salvador, J. J. Dannenberg, S. Dapprich, A. D. Daniels, Ö. Farkas, J. B. Foresman, J. V. Ortiz, J. Cioslowski, D. J. Fox, Gaussian, Inc., Wallingford CT, 2009; b) See Supporting Information file for a detailed description of the methods.
[18] M. H. Habicht, F. Wossidlo, T. Bens, E. A. Pidko, C. Müller, *Chem. Eur. J.* **2018**, *24*, 944.
[19] M. P. Mitoraj, A. Michalak, T. Ziegler, *J. Chem. Theory Comput.* **2009**, *5*, 962.
[20] a) G. A. Ardizzoia, S. Brenna, *Phys. Chem. Chem. Phys.* **2017**, *19*, 5971; b) L. Zhao, M. Hermann, W. H. E. Schwarz, G. Frenking, *Nat. Rev. Chem.* **2019**, *3*, 48.
[21] N. Mézailles, L. Ricard, F. Mathey, P. Le Floch, *Eur. J. Inorg. Chem.* **1999**, 2233.
[22] A. M. Echavarren, A. S. K. Hashmi, F. D. Toste, *Adv. Synth. Catal.* **2016**, *358*, 1347.
[23] a) A. S. K. Hashmi, G. J. Hutchings, *Angew. Chem. Int. Ed.* **2006**, *45*, 7896; *Angew. Chem.* **2006**, *118*, 8064; b) A. S. K. Hashmi, *Chem. Rev.* **2007**, *107*, 3180; c) N. Marion, S. P. Nolan, *Chem. Soc. Rev.* **2008**, *37*, 1776; d) D. J. Gorin, B. Sherry, F. D. Toste, *Chem. Rev.* **2008**, *108*, 3351; e) A. S. K. Hashmi, M. Rudolph, *Chem. Soc. Rev.* **2008**, *37*, 1766; f) M. Rudolph, A. S. K. Hashmi, *Chem. Soc. Rev.* **2012**, *41*, 2448.
[24] E. Jiménez-Núñez, A. M. Echavarren, *Chem. Rev.* **2008**, *108*, 3326.
[25] R. Dorel, A. M. Echavarren, *Chem. Rev.* **2015**, *115*, 9028.
[26] a) M. A. Tarselli, M. R. Gagné, *J. Org. Chem.* **2008**, *73*, 2439; b) S. Suárez-Pantiga, C. Hernández-Díaz, M. Piedrafita, E. Rubio, J. M. González, *Adv. Synth. Catal.* **2012**, *354*, 1651; c) N. Delpont, I. Escofet, P. Pérez-Galán, D. Spiegl, M. Raducan, C. Bour, R. Sinisi, A. M. Echavarren, *Catal. Sci. Technol.* **2013**, *3*, 3007; d) M. C. B. Jaimes, F. Rominger, M. M. Pereira, R. M. B. Carrilho, S. A. C. Carabineiro, A. S. K. Hashmi, *Chem. Commun.* **2014**, *50*, 4937.
[27] a) C. Nieto-Oberhuber, M. P. Muñoz, E. Buñuel, C. Nevado, D. J. Cárdenas, A. M. Echavarren, *Angew. Chem. Int. Ed.* **2004**, *43*, 2402; *Angew. Chem.* **2004**, *116*, 2456; b) C. Nieto-Oberhuber, S. López, A. M. Echavarren, *J. Am. Chem. Soc.* **2005**, *127*, 6178; c) N. Mézailles, L. Ricard, F. Gagosz, *Org. Lett.* **2005**, *7*, 4133; d) C. Nieto-Oberhuber, M. P. Muñoz, S. López, E. Jiménez-Núñez, C. Nevado, E. Herrero-Gómez, M. Raducan, A. M. Echavarren, *Chem. Eur. J.* **2006**, *12*, 1677.
[28] a) M. Freytag, S. Ito, M. Yoshifuji, *Chem. Asian J.* **2006**, *1*, 693; b) S. Ito, S. Kusano, N. Morita, K. Mikami, M. Yoshifuji, *J. Organomet. Chem.* **2010**, *695*, 291; c) S. Ito, L. Zhai, K. Mikami, *Chem. Asian J.* **2011**, *6*, 3077.
[29] a) A. S. K. Hashmi, J. P. Weyrauch, W. Frey, J. W. Bats, *Org. Lett.* **2004**, *6*, 4391; b) A. S. K. Hashmi, M. Rudolph, S. Schymura, J. Visus, W. Frey, *Eur. J. Org. Chem.* **2006**, 4905; c) A. S. K. Hashmi, A. Loos, A. Littmann, I. Braun, J. Knight, S. Doherty, F. Rominger, *Adv. Synth. Catal.* **2009**, *351*, 576; d) S. Doherty, J. G. Knight, A. S. K. Hashmi, C. H. Smyth, N. A. B. Ward, K. J. Robson, S. Tweedley, R. W. Harrington, W. Clegg, *Organometallics* **2010**, *29*, 4139; e) A. S. K. Hashmi, A. Loos, S. Doherty, J. G. Knight, K. J. Robson, F. Rominger, *Adv. Synth. Catal.* **2011**, *353*, 749; f) A. S. K. Hashmi, M. C. B. Jaimes, A. M. Schuster, F. Rominger, *J. Org. Chem.* **2012**, *77*, 6394; g) L. Biasiolo, D. Zotto, D. Zuccaccia, *Organometallics* **2015**, *34*, 1759.
[30] a) B. Schmid, L. M. Venanzi, A. Albinati, F. Mathey, *Inorg. Chem.* **1991**, *30*, 4693; b) A. Campos-Carrasco, L. E. E. Broeckx, J. J. M. Weemers, E. A. Pidko, M. Lutz, A. M. Masdeu-Bultó, D. Vogt, C. Müller, *Chem. Eur. J.* **2011**, *17*, 2510; c) I. de Krom, L. E. E. Broeckx, M. Lutz, C. Müller, *Chem. Eur. J.* **2013**, *19*, 3676.
[31] D. J. Gorin, F. D. Toste, *Nature* **2007**, *446*, 395.
[32] a) R. H. Hertwig, W. Koch, D. Schröder, H. Schwarz, J. Hrušák, P. Schwerdtfeger, *J. Phys. Chem.* **1996**, *100*, 12253; b) M. S. Nechaev, V. M. Rayón, G. Frenking, *J. Phys. Chem. A* **2004**, *108*, 3134.
[33] S. Doherty, J. G. Knight, D. O. Perry, N. A. B. Ward, D. M. Bittner, W. McFarlane, C. Wills, M. R. Probert, *Organometallics* **2016**, *35*, 1265.

Manuscript received: February 28, 2019
Accepted manuscript online: April 17, 2019
Version of record online: May 21, 2019

 © 2019 Wiley-VCH Verlag GmbH & Co. KGaA, Weinheim